Atomic and electronic structure of silicate adlayers on polar hexagonal SiC surfaces

Wenchang Lu, Peter Krüger, and Johannes Pollmann
Institut für Theoretische Physik II-Festkörperphysik, Universität Münster, Wilhelm-Klemm-Straße 10, D-48149 Münster, Germany
(Received 18 August 1999)

Structural and electronic properties of silicate adlayers on $(\sqrt{3}\times\sqrt{3})R30°$-reconstructed C-terminated $(000\bar{1})$ and Si-terminated (0001) surfaces of hexagonal 6*H*-SiC have been studied using the *ab initio* pseudopotential supercell method. Two significantly different structural models, previously suggested on the basis of a quantitative low-energy electron diffraction (LEED) analysis for the two adsorbate systems, have been investigated. Both of these models have been considered for both surfaces and the four respective structures have been optimized by total energy minimization calculations. The two structures with the lowest formation energy confirm the interpretation of the LEED data. In addition, they allow us to address the physical origin of the distinctly different reconstruction models for the two surfaces. The electronic structure of these surfaces according to local density approximation calculations is presented and discussed. Both models yield a number of oxygen-induced bound states and resonances within the projected valence band region and a band of localized dangling-bond states within the projected gap. Within the local density approximation, this dangling-bond band turns out to be half-filled in both cases, giving rise to metallic surfaces in contradiction to experiment. Therefore, the systems have also been studied within the framework of the Hubbard model and by employing the local-spin-density approximation. In both cases semiconducting surfaces are obtained in agreement with experiment. The dangling-bond bands resulting within the Hubbard-model calculation, in particular, are in quantitative agreement with most recent angle-resolved photoemission spectroscopy data for a Si_2O_3 silicate adlayer on SiC$(000\bar{1})$.

I. INTRODUCTION

The paramount technological potential of SiC for high-power, high-temperature, and high-frequency electronic devices[1] has led to a very strong interest in its bulk and surface properties both in experiment[2,3] and theory.[4] The formation of a high-quality insulating oxide layer on SiC, for example, is a key requirement for any metal-oxide–semiconductor device based on this new semiconductor material. Ordered oxide layers on hexagonal SiC surfaces have attracted particular attention. Preparing oxide layers on SiC, e.g., by thermal oxidation at high temperature,[5] by low-temperature remote plasma assisted oxidation,[6] or by oxidation of polycrystalline silicon on SiC,[7] leads to interfaces with a high defect density. On the other hand, it has been shown very recently that the preparation of hexagonal SiC surfaces by hydrogen plasma or etching in hydrogen flow produces highly ordered monolayers of silicon dioxide.[8] A microscopic understanding of the atomic structure and the bonding arrangements of such ultrathin oxide layers on hexagonal SiC surfaces is of prime interest, therefore.

Starke and co-workers[8,9] have experimentally investigated structural properties of ultrathin oxide layers on 6*H*-SiC$(000\bar{1})$ and 6*H*-SiC(0001). The authors have found, as noted above, a way to prepare well-defined epitaxial oxide monolayers on these surfaces. Well-ordered $(\sqrt{3}\times\sqrt{3})R30°$-reconstructed surfaces have been obtained. A quantitative low-energy electron diffraction (LEED) analysis could be achieved for Si_2O_3 silicate adlayers on top of otherwise bulk-truncated SiC surfaces. On the C-terminated $(000\bar{1})$ surface, the Si atoms of the silicate adlayer are bound directly to the C atoms of the substrate surface layer, thus forming Si-C bonds. We label this structure as the *Si_2O_3 model*, for brevity. On the Si-terminated (0001) surface, the Si adatoms are bound to the topmost substrate-surface Si layer via a linear oxygen bridge consisting of Si-O-Si. We label this structure as the *Si_2O_5 model*. Both the observed bond angles and bond lengths[8,9] agree well with those of bulk SiO_2. Potentially, ultrathin oxide layers may serve as a seed for the epitaxial growth of SiO_2 on the SiC surface. The lattice mismatch between these two crystals is only 5% while the respective mismatch between Si and SiO_2 amounts to 25%. Starke and co-workers[8,9] have also found that their oxide surfaces were stable in air, which is consistent with related observations of Bermudez.[10] In a more recent publication Hollering *et al.*[11] report electronic states of an ordered oxide on the C-terminated SiC$(000\bar{1})$ surface that they have prepared by annealing the above-mentioned samples[8,9] at 650 °C.

To the best of our knowledge there has been no theoretical investigation of the geometrical and electronic structure of silicate adlayers at hexagonal 6*H*-SiC surfaces so far. Therefore, in this paper we present and discuss the results of *ab initio* pseudopotential calculations for ultrathin oxide layers on 6*H*-SiC$(000\bar{1})$ and 6*H*-SiC(0001) surfaces in comparison with recent experimental data. We have energy-optimized the two above-mentioned structural models for both of these surfaces and have identified their relative stabilities. Detailed investigations of the electronic properties of these systems have been carried out in the framework of the local density approximation (LDA), as well as the local spin-density approximation (LSDA) of density functional theory[12] and on the basis of the Hubbard model.[13] Our structural results constitute an independent theoretical confirmation of

the LEED analysis and our electronic structure allows for an interpretation of most recent experimental results from angle-resolved photoemission spectroscopy [11](ARUPS).

The paper is organized as follows. In Sec. II we briefly describe the theoretical method. Section III presents and discusses structural and electronic properties of the silicate-covered C-terminated SiC$(000\bar{1})$ surface. Section IV is devoted to the presentation of our results for the silicate-covered Si-terminated SiC(0001) surface. In both cases, we identify the influence of coadsorbed hydrogen on the structural and electronic properties of the systems as well. A short summary concludes the paper in Sec. V.

II. CALCULATIONAL METHOD

Ab initio pseudopotential calculations are carried out within the LDA and LSDA. Nonlocal, norm-conserving pseudopotentials[14–17] in separable form, as suggested by Kleinman and Bylander,[18] and the exchange and correlation functional of Ceperley and Alder,[19] as parametrized by Perdew and Zunger,[20] are employed in our calculations. The wave functions are expanded in terms of linear combinations of Gaussian orbitals with s, p, d, and s^* symmetry. A detailed description of the method has been given in two previous papers.[21,22] Here we just give some additional information that is of particular relevance for the present systems. The basis states for Si, C, and H are the same as in Ref. 22. For the oxygen adatoms, we use 30 Gaussian orbitals with decay constants of 0.34, 0.95, and 2.72 (in atomic units). Six $\mathbf{k}_\parallel$ points in the irreducible part of the surface Brillouin zone turn out to be sufficient for the $(\sqrt{3}\times\sqrt{3})$ unit cell in order to obtain converged results. A supercell including the adlayers, eight SiC layers, and six vacuum layers is used to describe the surface system. The atoms in the first three substrate-surface layers and those in the adlayers are relaxed in order to eliminate the forces. The structure optimization is terminated when each force is less than 10^{-3} Ry/a.u. To guarantee a reliable identification of surface resonances within the energy region of the projected bulk bands we enlarge the slab by including 20 additional SiC bulk layers and calculate the surface-band structure.

III. SILICATE ADLAYERS AT THE C-TERMINATED SiC$(000\bar{1})$ SURFACE

In this section, we address the atomic and electronic structure of the C-terminated SiC$(000\bar{1})$ surface covered by silicate adlayers and we address the effects of coadsorbed hydrogen, as well.

A. Atomic structure of silicate adlayers at SiC$(000\bar{1})$

In the experiment by Bernhardt *et al.*,[8] an ordered $(\sqrt{3}\times\sqrt{3})R30°$ phase was observed. The LEED pattern for this surface is practically free from background. Moreover, in the Auger electron spectroscopy (AES) data, a strong O_{KLL} peak and an oxidic fine structure of Si_{LVV} indicate the existence of Si-O bonds in the surface.[3,8,9] By fitting their LEED data, a model including a silicate monolayer on top of the SiC$(000\bar{1})$ surface was suggested by Starke and co-workers.[8,9] In this lattice configuration (the Si_2O_3 model),

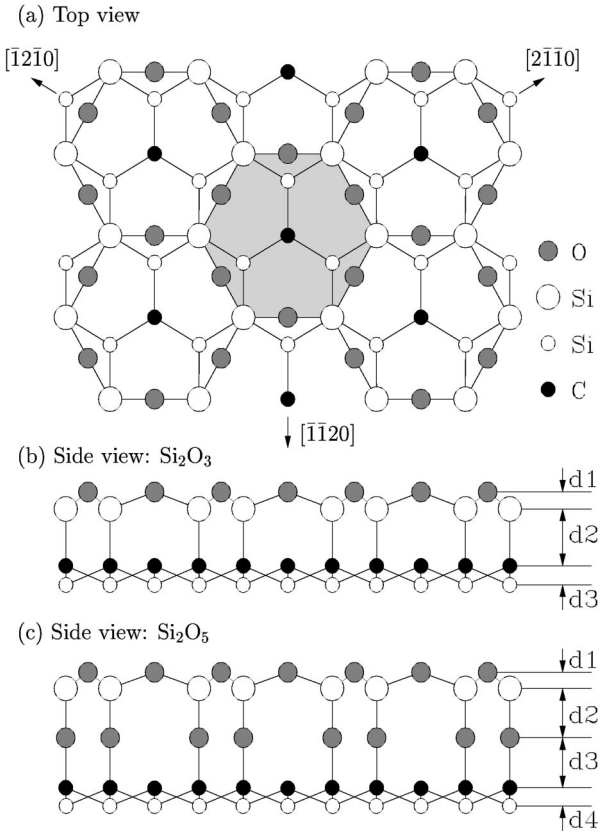

FIG. 1. Schematic (a) top and (b,c) side views of silicate adlayers on the 6*H*-SiC$(000\bar{1})$ surface. The side views show the (b) Si_2O_3 and (c) Si_2O_5 silicate layer model, respectively. The large open circles represent Si adatoms and the shaded circles represent oxygen adatoms in the silicate adlayer. The small open and solid circles represent the substrate-surface Si and C atoms. [To arrive at the respective models for the 6*H*-SiC(0001) surface, only the substrate-surface Si and C atoms need to be interchanged.] The normal distances between atomic layers are labelled d1, d2, d3 and d4. The dashed area in (a) represents the two-dimensional Wigner-Seitz cell.

there are two Si adatoms and three oxygen adatoms per surface unit cell. Figures. 1(a) and 1(b) show a schematic top and side view of this model. The Si-O-Si bonds at the surface are arranged in a honeycomb pattern (see the border line of the shaded area in the top view). Each oxygen atom is bound to two Si adatoms and its $n=2$ shell is fully saturated. Each Si adatom in the Si_2O_3 adlayer is fourfold coordinated. Three of its bonds are saturated by top-layer oxygen atoms while the fourth is involved in the tetrahedral bond to the substrate-surface layer C atoms. These bonds between the adlayer and the substrate-surface layer turn out to be usual Si-C bonds as in bulk SiC. The bond angles in the silicate adlayer are close to the tetrahedral angle. In each $(\sqrt{3}\times\sqrt{3})$ unit cell there is *one unsaturated dangling bond* at the substrate-surface layer C atoms staying in the center of the Si-O-Si honeycomb rings.

Since bulk 6*H*-SiC has the stacking sequence *ABCACB*, its $(000\bar{1})$ and (0001) surfaces can have three specific terminations. In the following, we use the same labels as suggested by Starke,[3] i.e., S1, S2 and S3 for *CACBA* . . . , *BCACB* . . . , and *ABCAC* . . . , respec-

TABLE I. Structure parameters for the C-terminated silicate-covered $6H$-SiC$(000\bar{1})$-$(\sqrt{3}\times\sqrt{3})R30°$ surface for the Si_2O_3 model with the three different surface terminations S1, S2, and S3, as well as, for the H-saturated S1 configurations (for details see text). Measured structure parameters from Starke and coworkers (Refs. 8 and 9) are given in parentheses.

Stacking type	S1	S2	S3	H-saturated
d_1	0.55 (0.55)	0.55 (0.54)	0.55	0.56
d_2	1.85 (1.91)	1.85 (1.87)	1.85	1.84
d_3	0.62 (0.58)	0.62 (0.60)	0.62	0.63
Downward	0.18 (0.08)	0.20 (0.19)	0.20	0.03
Si-O bond length	1.63 (1.64)	1.62 (1.63)	1.63	1.63
Si-O-Si angle	140.5° (140.8°)	140.4° (141.4°)	140.5°	139.9°
C-H bond length	-	-	-	1.17

tively. We have optimized the atomic structure of the Si_2O_3 model for all three types of termination S1, S2, and S3. The resulting structural parameters are listed in Table I. First we note that there are no significant differences between the layer distances and bond lengths for the three terminations. The vertical distance d_1 between Si and O sublayers in the silicate monolayer is 0.55 Å. The Si-O bond length of 1.62 Å and the Si-O-Si bond angle of 140.5° are very close to the respective values of 1.61 Å and 144° for α-quartz. The vertical distance $d_2=1.85$ Å is the bond length between the Si adlayer atoms and the C atoms on the top layer of the SiC substrate. It turns out to be very close to the bulk-bond length (1.89 Å) of SiC. The carbon atoms with the unsaturated dangling bond are shifted downward by 0.18–0.20 Å according to our calculations. The structural parameters from LEED experiments[8,9] are also listed in Table I for comparison. We find very good general agreement between our calculated results and the experimental data. Thus our results confirm the quantitative LEED analysis for this surface.[8,9]

Another conceivable model for this surface could be the Si_2O_5 structure suggested by Bernhardt *et al.*[9] for the silicate-covered Si-terminated SiC(0001) surface. The top view of the respective structure in the current case is the same as that for the Si_2O_3 model [see Fig. 1(a)] but its side view is different as shown in Fig. 1(c). There are two Si and five O adatoms in each unit cell. We call this configuration the Si_2O_5 model, therefore. For the current surface, the Si_2O_3 silicate adlayer is not directly bound to substrate-surface C atoms but it is connected to the substrate by a linear Si-O-C bridge [see Fig. 1(c)]. The Si-O and C-O bond lengths result as 1.59 Å and 1.39 Å, respectively. The former is close to the Si-O bond length of 1.61 Å in α-quartz, while the latter is approximately the sum of the covalent radii of C and O. Similar to the case of the Si_2O_3 model, the vertical distance d_1 between Si and O in the silicate adlayer is 0.54 Å and the distance d_4 between the topmost C and Si layers of the substrate turns out to be 0.63 Å. These values correspond to d_1 and d_3 in the Si_2O_3 model (see Table I).

To discern between the two considered structures, we have calculated the formation energies for both models using the method described in Refs. 22 and 23. For low values of the chemical potential of oxygen, μ_O, the Si_2O_3 model turns out to be more favorable while for larger values of μ_O the Si_2O_5 model has a slightly lower formation energy. There seems to be a fairly detailed balance between the energy of the involved bonds. In the Si_2O_3 model, there are six Si-O and two Si-C bonds per unit cell originating from the silicate adlayer. In the Si_2O_5 model, there are eight Si-O and two C-O bonds, respectively. To meaningfully compare the two systems, we have to add the bond energy of a free O_2 molecule in the former case. So leaving the six Si-O bonds within the silicate adlayer out of consideration (they are basically equal in both structures) the balance between one O-O and two Si-C bonds as compared to two Si-O and two C-O bonds determines the total energy difference. Close total energies for the two structures are conceivable, therefore. Since experiment[8,9,11] has clearly favored the Si_2O_3 model for the C-terminated surface and since ARUPS data[11] are available for that surface, we address the surface electronic structure for the Si_2O_3 model in the following subsection using our optimized surface configuration.

B. Electronic structure of Si_2O_3 at SiC$(000\bar{1})$

The calculated surface band structure of the C-terminated surface within the Si_2O_3 model is given in Fig. 2 together with the $(000\bar{1})$ projected bulk-band structure of $6H$-SiC. The latter is shown by the shaded areas. All bands plotted in the figure as full or dotted lines are related to surface bound states or resonances that mainly originate from the Si_2O_3 adlayer. The contribution from the adlayer atoms and the substrate-surface bilayer to the respective states is more than 40%. In the following discussion, we refer all energies to the valence band maximum (VBM) of the bulk crystal as energy zero ($E_{VBM}=0$). The three bands near -20 eV mainly originate from the $2s$ states of the oxygen adatoms contributing more than 80% to the respective states. Related to the C_{3v} symmetry, there is one singlet and one doublet state at the high symmetry points Γ and K. The bands located energetically between -7 and -10 eV are mainly derived from O $2p$ states. These bands are located partially in the ionic band gap. Between -1.8 eV and -4.0 eV, there are resonant bands resulting mainly from the Si$3p$–O$2p$ hybridized states in the Si-O-Si honeycomb ring.

In spite of the fact that all bonds of the Si and O atoms in the silicate adlayer are saturated, there is a fairly flat band of surface states in the fundamental band gap near 0.2 eV above E_{VBM}, in addition. Inspection of the respective wave functions shows that this flat band originates from the dangling

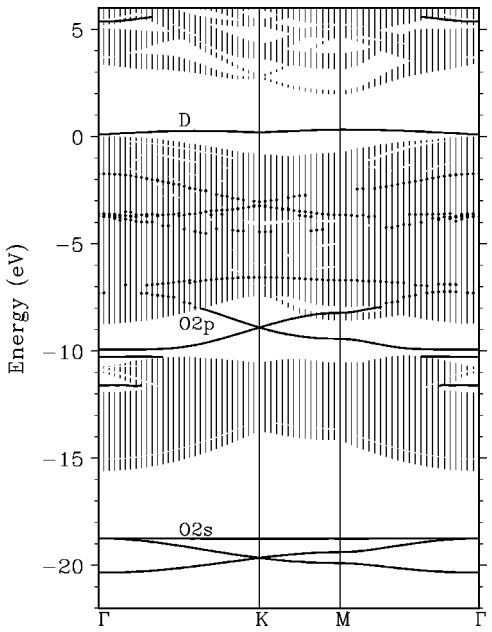

FIG. 2. Surface band structure of the Si_2O_3 model for the $6H$-SiC(0001)-$(\sqrt{3}\times\sqrt{3})R30°$ surface (see Fig. 1 for the structure). Surface-state and -resonance bands are shown by full and dotted lines, respectively. They are included in the figure if the adlayer atoms and substrate-surface bilayer atoms contribute more than 40% to the respective features. The shaded area represents the (0001) projected band structure of bulk $6H$-SiC.

bonds of the C atoms in the centers of the Si-O-Si honeycomb rings at the substrate surface. We label the band as D in the figure. The lateral distance between neighboring dangling bonds is fairly large (5.3 Å) and their interaction is screened by the silicate adlayer. In consequence, the upward dispersion of the D band from the surface Brillouin zone center (Γ point) to its corners (K and M point) is small. Since there is one unsaturated dangling bond per surface unit cell, the dangling-bond band is half-filled. Thus our LDA calculations yield a metallic surface while experiment observes a semiconducting surface.[11]

To resolve this discrepancy and contribute to a better understanding of the electronic properties of this system we have carried out spin-polarized local density calculations to better describe the ground state properties of our system, and we have employed the Hubbard model[13] in order to approximately describe excitations, in addition. The correlation energy U of two electrons in the dangling bonds is taken as a parameter determined from our LDA calculations for different occupations of the dangling bonds. Northtrup and Neugebauer,[24] Furthmüller *et al.*,[25] and Rohlfing and Pollmann[26] have demonstrated that such Hubbard-model calculations can account for the photoemission[27] and inverse photoemission[28] spectra of the clean SiC(0001)-$(\sqrt{3}\times\sqrt{3})R30°$ surface. Thus it is to be expected that the Hubbard model applies to the current system, as well.

The LSDA calculations have been started with a ferromagnetic configuration, i.e., all electrons in the dangling bonds occupy the spin-up state. During the self-consistency cycle this configuration remains stable, with a total energy gain of 0.12 eV per dangling bond due to the spin polarization. A section of the band structure including the dangling-bond bands is shown in Fig. 3(a) for the LDA (see Fig. 2 for comparison) and in Fig. 3(b) for the LSDA calculation. Within LDA, the dangling-bond band D is half-filled. It splits by 0.6 eV into two bands in the fully spin-polarized LSDA calculation. The lower band is completely occupied while the upper one is empty. We label them as $D\uparrow$ and $D\downarrow$, respectively. Thus the surface results as semiconducting in the LSDA. The calculated gap energy of 0.6 eV, however, is considerably smaller than the measured gap energy of about 1.4 eV.[11] This kind of deviation in gap energies is typical for local (spin) density calculations. The one-particle LSD theory underestimates the band gap by a considerable amount. In order to arrive at a correct description of the band gap, quasiparticle band-structure calculations beyond LSDA, e.g., within the *GW* approximation[29] would be useful but they are very demanding.[26]

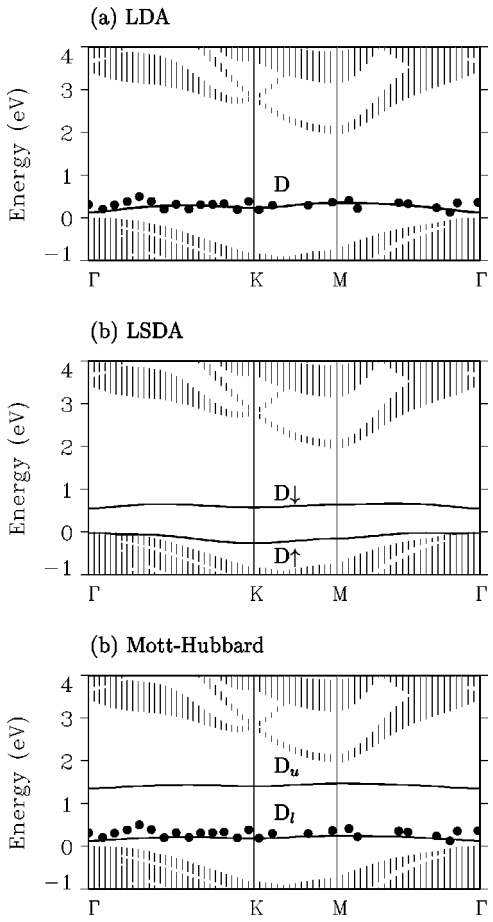

FIG. 3. Section of the surface-band structure for the Si_2O_3 model of $6H$-SiC(0001)-$(\sqrt{3}\times\sqrt{3})R30°$ including the dangling-bond bands. The upper, middle, and bottom panels show the results from LDA, LSDA, and Hubbard-model calculations, respectively. The shaded area is the (0001) projected band structure of bulk $6H$-SiC. The solid dots represent ARUPS data from Ref. 11.

To improve on this aspect the concept of a Mott-Hubbard metal-insulator transition[13] may be used as an alternative to more appropriately describe excited states and the dangling-bond band splitting. When the intra-atomic Coulomb interaction U is much larger than the respective bandwidth, the half-filled LDA band splits into two bands with half the width of the original band and an energetic separation of U. The lower Hubbard band (D_l) is fully occupied while the

upper Hubbard band (D_u) is empty. The surface changes from a metallic to an insulating phase by a Mott-Hubbard transition. To calculate the Coulomb interaction U, we use the charged supercell approach.[24,30] The unit cell of the oxygen-covered surface was enlarged to a 3×3 cell in which all C dangling bonds except one are saturated by hydrogen to simulate isolated C dangling bonds. The total energy of the system has been calculated for various possible charged states of the dangling bonds, as suggested by Northrup and Neugebauer.[24] The resulting value for the intra-atomic Coulomb interaction U is 1.2 eV. The lower and upper Hubbard bands are plotted in Fig. 3(c). The lower band has only half of the dispersion of the LDA band D and its center of energy resides at the same energy position as that of the D band. Due to the large splitting and small band width, there is no overlap between the lower and upper Hubbard bands. This results in a semiconducting surface as in our spin-polarized calculation. But now the surface band gap is about two times as large as in the LSDA results. The calculated band gap of 1.2 eV compares favorably with the experimental surface gap of about 1.4 eV as clearly observed in the band bending of the annealed surface.[11] The agreement is good in view of the fact that the error in the Hubbard U as calculated by the above procedure is as large as several tenths of an eV.[24]

For a direct comparison with experiment, we have included the ARUPS data for the most salient surface-state band D in Figs. 3(a) and 3(c). We observe that the agreement for the occupied dangling-bond band is very good in both cases. From the LDA calculation, however, we obtain only one half-filled band. So the energy position of the occupied and the empty surface states essentially coincide and the surface is metallic, in addition. These results contradict the experimental observations.[11] Within the Hubbard model [see Fig. 3(c)], in contrast, we obtain the fully occupied band D_l in very good agreement with the ARUPS data and the empty band D_u that pins the Fermi level of an n-doped sample some 1.2 eV above the D_l band. Thus the surface is obviously semiconducting. All these findings are in accord with the data of Hollering *et al.*[11]

In order to get some information on possible magnetic orderings of the spins at the surface we have also carried out LSDA calculations investigating an antiferromagnetic (AFM) configuration. For the two-dimensional triangular lattice there are many possibilities for an AFM arrangement. Here we consider one simple example. All electrons in rows along the $[2\bar{1}\bar{1}0]$ direction are assumed to occupy the same spin state, while those in rows along the $[\bar{1}\bar{2}\bar{1}0]$ or $[\bar{1}\bar{1}20]$ directions are assumed to occupy the opposite spin states, respectively. Thus each site has two neighboring sites with electrons of the same spin and four neighboring sites with electrons having opposite spin. This type of an antiferromagnetic structure turns out to be stable. The total energy difference between the ferromagnetic and this antiferromagnetic configuration is less than 5 meV and there is no significant difference for the corresponding band structures. This simply results from the fact that the distance between neighboring dangling bonds is as large as 5.3 Å and their interaction is correspondingly small. The screening effect of the silicate adlayer reduces the interaction between the dangling bonds, in addition. This very small interaction may lead to a random occupation of the spin-up and spin-down orbitals. Therefore, the surface will presumably show neither a ferromagnetic nor an antiferromagnetic phase, but will show a paramagnetic phase at room temperature or above.

C. Effects of coadsorbed hydrogen

Starke and co-workers[8,9] have observed that the samples prepared in their experiments were stable in air. The existence of dangling bonds certainly would be unfavorable for a stable surface structure in air. Since the samples were treated either thermally by annealing in hydrogen flow or by a hydrogen plasma,[8,9] one can expect that the abundantly available H atoms have saturated the existing dangling bonds in the samples. We have considered geometries with one hydrogen atom added per $(\sqrt{3}\times\sqrt{3})$ unit cell also, therefore. By keeping the H atoms on top of the C atoms in the center of each Si-O-Si honeycomb ring saturating the C dangling bonds, the structure was optimized anew. The resulting structure parameters are shown in Table I, as well. Since the stacking sequence has a negligible effect on the structure parameters of the H-covered surfaces, we only show the parameters for H coadsorbed at the stacking sequence S1. Comparing the respective results with the structure parameters of the surface without H saturation, we can clearly see the following: The H saturation affects the Si-O bond length and the Si-O-Si bond angle in the silicate bilayer only marginally. The only noteworthy change concerns the downward shift of the C atoms in the center of the Si-O-Si honeycomb rings. After the H atoms saturate the dangling bonds, the downward displacement decreases from 0.18 Å to 0.03 Å. This marginal influence of the coadsorbed H on the structure explains why Starke and co-workers[8,9] and Hollering *et al.*[11] have observed basically the same atomic structure at room temperature and at annealing temperature, i.e., with and without the coadsorbed hydrogen.

The calculated band structure for the hydrogen-saturated surface (not shown here for the sake of brevity) exhibits no surface or interface states in the fundamental band gap in agreement with the data.[11] This fact obviously occurs because the H atoms saturate the dangling bonds of the C atoms in the center of Si-O-Si honeycomb rings and fully passivate the surface. The other bands within the bulk valence-band projection remain similar to those for the S1 configuration without H saturation (cf. Fig. 2). Our results confirm that hydrogen adsorption on the oxide surface is very important for reducing the density of midgap states at the adsorbate-substrate interface. This is in accord with high-temperature annealing in a H_2-containing ambient,[6] which was observed to reduce the defect density at the oxidized SiC surface drastically from 10^{13} to $10^{11}\,\mathrm{cm}^{-2}$.

IV. SILICATE ADLAYERS AT THE Si-TERMINATED SiC(0001) SURFACE

In this section, we address the atomic and electronic structure of the Si-terminated SiC(0001) surface covered by silicates as well as by coadsorbed hydrogen.

A. Atomic structure of silicate adlayers at SiC(0001)

For the silicate-covered (0001) surface, LEED and AES analyses also indicate the existence of Si-O-Si honeycomb

TABLE II. Structure parameters of the Si-terminated silicate-covered 6*H*-SiC(0001)-($\sqrt{3}\times\sqrt{3}$)*R*30° surface for the Si_2O_5 model with the three different surface terminations S1, S2, and S3 as well as, for the H-saturated S1 configurations (for details see text). Measured structure parameters from Starke and co-workers (Refs. 8 and 9) are given in parentheses.

Stacking type	S1	S2	S3	H-saturated
d_1	0.52	0.53	0.52	0.53
d_2	1.60 (1.57)	1.60 (1.57)	1.60 (1.57)	1.60
d_3	1.62 (1.63)	1.62 (1.63)	1.62 (1.63)	1.63
d_4	0.59	0.59	0.59	0.58
Downward	0.003	0.01	0.02	-0.06
Si-O bond length	1.62 (1.61)	1.62 (1.61)	1.62 (1.61)	1.62
Si-O-Si angle	142.6° (146°)	142.2° (146°)	142.2° (146°)	142.2°
Si-H bond length	-	-	-	1.55

rings in the top layer. From their data Starke *et al.*[9] have derived the Si_2O_5 model for this surface. The respective structure is shown in Figs. 1(a) and 1(c) if the C and Si atoms in the SiC bilayer on top of the substrate surface are interchanged. The Si-O-Si ring in the unit cell is not directly bound to Si substrate-surface atoms via a Si-Si bond but rather by a linear Si-O-Si bridge in normal direction to the surface [see Fig. 1(c)]. The structural parameters for the optimized geometry as resulting from our calculations are listed in Table II together with the experimental values. For the different terminations of the stacking sequences S1, S2, and S3, there is no significant difference between the layer distances and bond lengths. In the top bilayer, i.e., the Si-O-Si honeycomb ring, the interlayer distance is 0.52 Å and the oxygen atoms reside on the top. The resulting Si-O bond length of 1.62 Å and the Si-O-Si angle of 142° are very close to the respective values in α-quartz. In the substrate-surface SiC bilayer, the interlayer distance (0.59 Å) is compressed by 6% relative to the respective value in bulk SiC. There is one substrate-surface Si atom in each unit cell in the center of the honeycomb ring having an unsaturated dangling bond. Comparing our optimized parameters with the experimental results,[9] we find equally good agreement for all three terminations S1, S2, and S3. Thus also in this case, our theoretical study corroborates the model suggested by Starke and co-workers[8,9] on the basis of their experimental data.

We have also considered the Si_2O_3 model for the Si-terminated substrate surface [see Figs. 1(a) and 1(b) and interchange C and Si atoms in the top bilayer of the substrate]. This model has Si-Si bonds between the silicate adlayer and the substrate surface Si atoms. Calculation of the formation energy shows that this model is much less stable than the Si_2O_5 model in the whole range of the allowed oxygen chemical potential μ_O. In the limit of $\mu_O = 0.5E_O$ (where E_O is the total energy of an O_2 molecule), the formation energy difference is as large as 10 eV per unit cell. The respective consideration as in Sec. III A shows in this case that the bond energies to be compared are those of one O-O and two Si-Si bonds for the Si_2O_3 model with those of four Si-O bonds for the Si_2O_5 model. Within this simple reasoning one would expect the latter model to be much more stable than the former for the Si-terminated (0001) surface. These findings are consistent with the results of the LEED experiments,[8,9] which have led the authors to their Si_2O_5 model. In the following, we will only discuss the electronic structure of the latter model, therefore.

B. Electronic structure of Si_2O_5 at SiC(0001)

The respective surface band structure is shown in Fig. 4. The shaded area represents the (0001)-projected band structure of the bulk 6*H*-SiC crystal. The 2*s* states of the five oxygen adatoms per unit cell give rise to five bands around -20 eV with a total bandwidth of 2.0 eV. In the ionic band gap, there are O2*p*–related bands. The Si-O bonds give rise to surface resonances between -2 and -4 eV. These three groups of bands are characteristic for the silicate adsorption and are shown in Figs. 2 and 4. The very flat band at 1.2 eV above E_{VBM} stems from the dangling bonds at the substrate-surface Si atoms in the center of the Si-O-Si honeycomb rings. The band occurs about 1 eV higher in energy than the respective band at the $(000\bar{1})$ surface (see Fig. 2 for com-

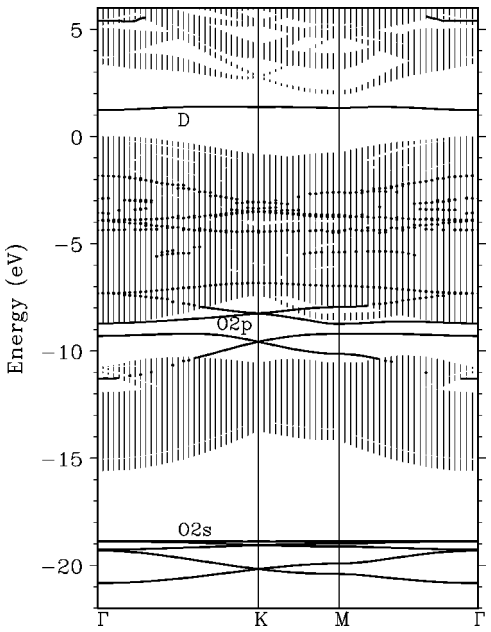

FIG. 4. Surface-band structure of the Si_2O_5 model for the 6*H*-SiC(0001)-($\sqrt{3}\times\sqrt{3}$)*R*30° surface (see Fig. 1 for the structure and see also the caption of Fig. 2).

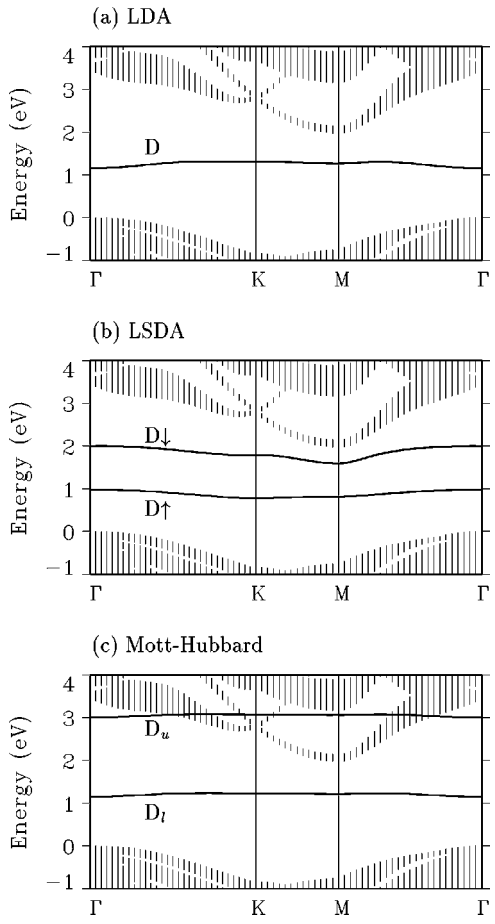

FIG. 5. Section of the surface-band structure for the Si_2O_5 model of $6H$-SiC(0001)-$(\sqrt{3}\times\sqrt{3})R30°$ including the dangling bond bands. The upper, middle, and bottom panels show the results from LDA, LSDA, and Hubbard-model calculations, respectively.

parison). This difference stems from the fact that the C potential is stronger than the Si potential. Thus the C dangling-bond band (Fig. 2) is lower in energy than the Si dangling-bond band in Fig. 4. Similar to the case of the C-terminated $(000\bar{1})$ surface, this dangling-bond band turns out to be half-filled in our LDA results.

Consequently, we have carried out spin-polarized local density and Hubbard-model calculations for this surface, as well, in order to investigate the electronic properties of the dangling-bond state. The dangling-bond bands calculated within LDA, LSDA, and the Hubbard model are shown in Fig. 5. In the LSDA calculation, the spin arrangement can be either ferromagnetic or antiferromagnetic. Our calculations for both arrangements show that the total energy difference is less than 2 meV per $(\sqrt{3}\times\sqrt{3})$ unit cell and that the band structures are very similar with the same value of spin splitting. Therefore, only the band structure for the ferromagnetic arrangement is displayed in the figure. The splitting between the spin-up and spin-down bands at the Γ point is 1.0 eV. Because of the very small dispersion of the $D\uparrow$ and $D\downarrow$ bands, there is no overlap between these two bands. The spin-up band $D\uparrow$ is fully occupied and the spin-down band $D\downarrow$ is empty. In consequence the surface is semiconducting.

Similar to the C-terminated surface, we have also studied the band splitting by employing the Hubbard model. Our calculated Hubbard U for this surface is 1.8 eV. Therefore, the half-filled LDA band D splits into two bands D_u and D_l separated by an energy gap of 1.8 eV. It is interesting to note at this point that the intra-atomic Coulomb interaction energy U of the Si dangling bonds at the silicate-covered SiC(0001) surface turns out to be close to the respective values obtained for the clean Si-terminated SiC(0001)-$(\sqrt{3}\times\sqrt{3})R30°$ surface by Northrup and Neugebauer[24] (1.6 eV), Furthmüller *et al.*[25] (2.1 eV), and Rohlfing and Pollmann[26] (1.95 eV). For the clean surface we obtain as well $U=1.8$ eV, when the calculations are carried out as desribed in this work. The close agreement of the Hubbard U values resulting from four different calculations certainly stems from the fact that in each case we are dealing with the Coulomb-correlation energy of the same unsaturated localized Si dangling bond.

To the best of our knowledge, there are no ARPES data available for the silicate-covered Si-terminated $6H$-SiC(0001)-$(\sqrt{3}\times\sqrt{3})R30°$, so far.

C. Effects of coadsorbed hydrogen

Saturation of the Si dangling bond in the center of the Si-O-Si honeycomb rings by hydrogen basically does not change all but one structural parameter (see Table II). Only the vertical position of the substrate-surface Si atoms is marginally changed. As our calculations have shown, without adsorbed hydrogen the Si atoms with a dangling bond are shifted downward by 0.003 Å with respect to the other substrate-surface Si atoms for the S1 termination. When hydrogen is adsorbed saturating the dangling bonds, these atoms are shifted upwards by 0.06 Å. The band structure for the H-terminated S1 configuration shows no significant change below E_{VBM}, as compared to Fig. 4. Only the dangling-bond band D in the projected bulk-band gap disappears. Similar to the C-terminated surface, this also indicates for the current system that the interface density of states is drastically reduced by hydrogen saturation. When all Si dangling bonds are saturated, this surface should also be stable in air as has been observed in experiment.[8,9]

V. SUMMARY

Ab initio pseudopotential supercell calculations have been carried out for silicate adlayers at the $(\sqrt{3}\times\sqrt{3})R30°$-reconstructed $6H$-SiC$(000\bar{1})$ and $6H$-SiC(0001) surfaces. In the case of silicate-covered SiC$(000\bar{1})$ surfaces, both the Si_2O_3 and the Si_2O_5 models have roughly the same formation energy. In the case of the SiC(0001) surface, silicate adsorption within the Si_2O_5 model turns out to be energetically much more favorable than adsorption in the Si_2O_3 configuration. The calculated optimal structural parameters are in excellent agreement with the results of recent LEED experiments.[8,9] Generally, oxygen-derived $2s$ states have been obtained around 20 eV below the valence-band maximum for all the investigated structures. The O $2p$ states induce characteristic surface features in the ionic gap. These two groups of surface state bands can be considered as the ''fingerprints'' of the silicate adlayers. In all our LDA results, except for the surfaces with coadsorbed H, we find a half-filled dangling-bond band in the fundamental gap, in addition. For the C-terminated $(000\bar{1})$ surface, this band occurs near 0.2 eV above E_{VBM}.

For the Si-terminated (0001) surface, it resides near 1.1 eV above E_{VBM}. From our LDA calculations both surfaces result as metallic. In the outcome of our spin-polarized LSDA calculations, the dangling-bond band splits into two bands with a gap of 0.6 eV and 1.0 eV for the $(000\bar{1})$ and (0001) surface, respectively. Thus, the spin-polarized LSDA calculations already show that the considered surfaces are semiconducting. However, as is well-known, such calculations underestimate the value of the gap energy. To overcome these shortcomings and to include correlation effects at least in a model calculation, we have employed the Hubbard model for the energetically most stable configurations. Within the Hubbard model, a gap of 1.2 eV and 1.8 eV is found for the $(000\bar{1})$ and (0001) surfaces, respectively. For the silicate-covered SiC$(000\bar{1})$ surface our results for the dangling-bond bands in the energy gap have been compared with most recent ARUPS and band-bending data. Theory and experiment are found to be in very good agreement, indeed, lending further support to the atomic structure models and to the notion that correlation effects as described within the Hubbard model are very important for a quantitative interpretation of the data. Hydrogen saturation for both the $(000\bar{1})$ and (0001) surface clears the gap from surface states since the H atoms saturate the C or Si dangling bonds, respectively. This result supports the experimental finding that both surfaces are stable in air at room temperature.

ACKNOWLEDGMENTS

It is our great pleasure to thank Dr. U. Starke for fruitful discussions. In addition, we acknowledge financial support of this work by the Deutsche Forschungsgemeinschaft (Bonn, Germany) under Contract No. Po 215/13-2 and a grant of Cray computer time at the John von Neumann-Institute for Computing (NIC) of the Forschungszentrum Jülich (Germany) under Contract No. K2710000.

[1] H. Morkoç, S. Strite, G.B. Bao, M.E. Lin, B. Sverdlov, and M. Burns, J. Appl. Phys. **76**, 1363 (1994).
[2] V.M. Bermudez, Phys. Status Solidi B **202**, 447 (1997).
[3] U. Starke, Phys. Status Solidi B **202**, 475 (1997).
[4] J. Pollmann, P. Krüger, and M. Sabisch, Phys. Status Solidi B **202**, 421 (1997).
[5] L. Muehlhoff, M.J. Bozack, W.J. Choyke, and J.T. Yates, Jr., J. Appl. Phys. **60**, 2558 (1986).
[6] A. Gölz, G. Lucovsky, K. Koh, D. Wolfe, H. Niimi, and H. Kurz, J. Vac. Sci. Technol. B **15**, 1097 (1997).
[7] J. Tan, M.K. Das, J.A. Cooper, Jr., and M.R. Melloch, Appl. Phys. Lett. **70**, 2280 (1997).
[8] J. Bernhardt, J. Schardt, U. Starke, and K. Heinz, Appl. Phys. Lett. **74**, 1084 (1999).
[9] U. Starke, J. Schardt, J. Bernhardt, and K. Heinz, J. Vac. Sci. Technol. A **17**, 1688 (1999).
[10] V.M. Bermudez, Appl. Surf. Sci. **84**, 45 (1995).
[11] M. Hollering, F. Maier, N. Sieber, M. Stammler, J. Ristein, L. Ley, A.P.J. Stampfl, J.D. Riley, R.C.G. Leckey, F.P. Leisenberger, and F.P. Netzer, Surf. Sci. **442**, 531 (1999).
[12] W. Kohn and L.J. Sham, Phys. Rev. **140**, A1133 (1965).
[13] J. Hubbard, Proc. R. Soc. London, Ser. A **281**, 401 (1964).
[14] For the carbon and Si atoms (Ref. 15) and for the oxygen atoms (Ref. 16), very smooth pseudopotentials have been used to reduce the numerical effort. For H we employ the pseudopotential reported by Gygi (Ref. 17).
[15] M. Sabisch, P. Krüger, A. Mazur, M. Rohlfing, and J. Pollmann, Phys. Rev. B **53**, 13 121 (1996).
[16] M. Sabisch, Diploma thesis, Universität Münster, 1993.
[17] F. Gygi, Phys. Rev. B **48**, 11 692 (1993).
[18] L. Kleinman and D.M. Bylander, Phys. Rev. Lett. **48**, 1425 (1982).
[19] D.M. Ceperley and B.J. Alder, Phys. Rev. Lett. **45**, 566 (1980).
[20] J.P. Perdew and A. Zunger, Phys. Rev. B **23**, 5048 (1981).
[21] M. Sabisch, P. Krüger, and J. Pollmann, Phys. Rev. B **55**, 10 561 (1997).
[22] W. Lu, P. Krüger, and J. Pollmann, Phys. Rev. B **60**, 2495 (1999).
[23] J.E. Northrup and J. Neugebauer, Phys. Rev. B **52**, 17 001 (1995).
[24] J.E. Northrup and J. Neugebauer, Phys. Rev. B **57**, R4230 (1998).
[25] J. Furthmüller, F. Bechstedt, H. Hüsken, B. Schröter, and W. Richter, Phys. Rev. B **58**, 13 712 (1998).
[26] M. Rohlfing and J. Pollmann, Phys. Rev. Lett. **84**, 135 (2000).
[27] L.I. Johanson, F. Owman, and P. Martensson, Surf. Sci. Lett. **360**, L478 (1996).
[28] J.-M. Themlin, I. Forbeaux, V. Langlais, H. Belkhir, and J.-M. Debever, Europhys. Lett. **39**, 61 (1997).
[29] L. Hedin, Phys. Rev. **139**, A796 (1965).
[30] Y. Bar-Yam and J.D. Joannopoulos, Phys. Rev. Lett. **56**, 2203 (1986).